Synthesis of Polystyrene with Mixtures of Mono- and Bifunctional Initiators

I. M. GONZÁLEZ,[1] G. R. MEIRA,[2] and H. M. OLIVA[1,*]

[1] Facultad de Ingeniería, Universidad del Zulia, Apartado 4011A-526, Maracaibo, Venezuela, and
[2]INTEC (CONICET and Universidad Nacional del Litoral), Santa Fe (3000), Argentina

SYNOPSIS

This work studies the bulk and nonisothermic polymerization of styrene (S) using mixtures of mono- and bifunctional initiators. The effects on polymerization rate and on molecular weight averages after changes in the global initiator concentration and in the nature of the initiator mixtures were experimentally and theoretically analyzed. The mathematical model was adapted from the literature to admit initiator mixtures and to simulate the applied temperature profiles. Compared to the standard use of monofunctional initiators, the use of initiator mixtures that include bifunctional initiators presents the advantage of reducing the polymerization time, while not deteriorating the final polymer quality. The simulation program accurately describes the evolution of conversion, but exhibits some deviations with the average molecular weights. © 1996 John Wiley & Sons, Inc.

INTRODUCTION

The radical polymerization of S with initiator mixtures of different decomposition rates is a common industrial practice.[1,2] In recent publications, the use of bifunctional initiators has been suggested by several authors as a means of producing high molecular weight polystyrene (PS), at high polymerization rates.[2-8] Bifunctional initiators can also be applied to obtain block copolymers via two-step radical polymerizations.[6]

Simionescu and Popa[9] report on the synthesis of a new bifunctional radical initiator (cumyl 4-*t*-butylazo-4-cyanoperoxypentanoate) and its behavior in the polymerization process. This initiator was used in styrene polymerization and the conversion of the polymer studied in conection to monomer and initiator concentration, time of reaction, and temperature. With the multiple regression method, an equation correlating the PS conversion with the previously mentioned variables was established.

The presence of two peroxide groups per molecule in bifunctional initiators complicates the reaction kinetics because unreacted peroxides may be present in the growing chains and in the dead polymer molecules.[6]

In free-radical polymerizations, the reaction rate depends on the initiator concentration. With monofunctional initiators, the polymerization is of order 0.5 with respect to the initiator concentration.[10] Due to the reinitiation reactions, the kinetics with bifunctional initiators is more complex. For a biperoxide, the process may be illustrated by the following equations:[11]

Primary initiator descomposition:

$$R_1—O—O—R—O—O—R_2 \rightarrow R_1O^{\bullet} + R_2OORO^{\bullet}$$

Initiation:

$$R_2OORO^{\bullet} + M \rightarrow R_2OOROM^{\bullet}$$

Propagation:

$$R_2OOROM^{\bullet} + n - 1M \rightarrow R_2OOROM^{\bullet}_n$$

Reinitiation:

$$R_1OM_{n+m}OROOR_2 \rightarrow R_1OM_{n+m}ORO^{\bullet} + R_2O^{\bullet}$$

* To whom correspondence should be addressed.

Journal of Applied Polymer Science, Vol. 59, 1015–1026 (1996)
 CCC 0021-8995/96/061015-12

In the case of PS, termination is only by recombination. When bifunctional initiators are used, the dead polymer may contain zero, one, or two peroxide groups per molecule.

Several kinetic models have been proposed for the free-radical and isothermal polymerization of S with (symmetrical and nonsymmetrical) bifunctional initiators. For example, Kuchanov et al.[12] evaluated different mono-, bi-, and trifunctional initiators of similar structure, with a constant total peroxide concentration. They found similar polymerization rates, independently of the functionality. Villalobos et al.[5] investigated the polymerization of S with various commercial initiators. Yoon and Choi[6] studied the same kinetics, but with 2,5 dimethyl-2,5 bis (2 ethylhexanoyl peroxi) hexane (or L256). The model included the formation of primary birradicals, thermal initiation, and volume change along the polymerization. Villalobos et al.[5] theoretically and experimentally investigated the bulk polymerization of S with bifunctional initiators. Their main conclusions were: taking as reference polystyrene synthesis with the monofunctional initiator benzoyl peroxide at initiator concentration of 0.01 mol/l and 90°C, it was demonstrated that reductions in polymerization cycle time by 20 to 75% may be achieved by using bifunctional initiators at same or lower concentrations and at an adequate polymerization temperature. The simulation program created from the model developed by Villalobos[5] predicted quite accurately both the reaction rate and molecular weight distribution development. However, the predictions of molecular weight values tend to become poor at high monomer conversions.

This work experimentally and theoretically investigates the bulk polymerization of S, with the aim of evaluating the advantages of employing initiator mixtures that include bifunctional initiators. Based on six commercial initiators (three mono- and three bifunctional), all combinations involving: (a) two monofunctional, (b) one mono- and one bifunctional, and (c) two bifunctional initiators were evaluated. The effects on reaction rate and molecular weights were analyzed.

EXPERIMENTAL WORK

The initiator mixtures indicated in Table I were investigated. Every reaction employed two initiators: one of low-temperature decomposition (90°C), and another of high-temperature decomposition (120°C). In all cases, the molar ratio between the low- and the high-temperature initiator was fixed at 1.5:1. The reaction temperature profiles depend on the decomposition characteristics of the initiator mixtures, to provide a half-life time of approximately 1 h. All polymerizations involved an 8-h cycle, that was carried out as follows. First, the temperature was suddenly increased to 90°C and maintained at that value for 4 h. Then, a temperature ramp of 3°C/min was applied until 120°C or 135°C was reached. This temperature was maintained until completion of the cycle.

Table I Experimental Conditions and Global Results

Monofunctional Initiator			Bifunctional Initiator										
High-Temp.	Low-Temp.		High-Temp.		Low-Temp.	Init Conc.	Measurements		Predictions		% Deviation		Global
TBPA	BPO	TBPO	L118	L233	L256	mol/L	$\overline{M_n}$	$\overline{M_w}$	$\overline{M_n}$	$\overline{M_w}$	$\overline{M_n}$	$\overline{M_w}$	Effic.
X	X					0.01	91800	257000	101000	199000	−9.8	+22.5	0.53
X		X				0.01	99400	277000	97900	195000	+1.5	+29.5	0.57
	X		X			0.01	79600	207000	107000	221000	−34.4	−6.8	0.58
		X	X			0.01	99200	262000	95000	183000	+4.2	+30.1	0.57
	X			X		0.01	78600	202000	91700	183000	−16.7	+9.2	0.52
		X		X		0.01	91700	224000	89200	180000	+2.7	+19.6	0.57
			X		X	0.01	94000	282000	97400	220000	−3.7	+22.3	0.65
				X	X	0.01	86100	233000	90400	224000	−5.0	+4.5	0.64
X	X					0.016	66100	159000	77200	167000	−16.8	−5.4	0.52
X		X				0.016	88800	239000	87700	177000	+1.2	+25.9	0.47
	X		X			0.016	68800	165000	80100	167000	−16.4	−1.4	0.49
		X	X			0.016	80700	222000	69200	163000	+14.2	+26.7	0.50
	X			X		0.016	72300	167000	79100	166000	−9.7	+0.7	0.50
		X		X		0.016	79500	199000	82700	167000	−4.1	+16.1	0.50
			X		X	0.016	78100	276000	87600	222000	−12.2	+19.7	0.61
				X	X	0.016	71000	239000	107000	213000	−50.7	+10.7	0.62

As indicated in Table I, the global initiator concentration was either 0.01 or 0.016 mol/L. The employed monofunctional initiators were benzoyl peroxide (BPO), terbutylperoctoate (TBPO), and terbutylperacetate (TBPA), from Akzo Chemicals. The bifunctional initiators were 2,5 dimethyl-2,5 bis (2 ethyl hexanoyl peroxi) hexane (L256), 2,5 dimethyl-2,5 bis (benzoyl peroxy) hexane (L118), and ethyl 3,3 di (terbutyl peroxi) butirate (L233-M75), from Pennwalt Chemicals. All initiators were used as received, and their purity was determined following ASTMD 2340-82.

The reactions were carried out in 5 mm O.D. glass ampoules. The ampoules were previously purged and degassed through several cycles of freezing and thawing, using liquid nitrogen.

The polymerization cycle was initiated by introducing a set of glass ampoules into a thermostatic bath at 90°C. The bath was programmed to provide the required temperature profile. Samples were taken every hour and frozen in liquid nitrogen until their analysis. The polymer contents were dissolved in 1,4 dioxane, and precipitated in an excess of methanol. Then, the samples were vacuum dryed, and the conversion was gravimetrically determined. Finally, the molecular weight averages were determined from samples obtained at 8 h by means of a Dupont LC870 size exclusion chromatograph fitted with a set of PSM 60 and PSM1000S Zorbax columns.

The global results for all experiments and simulation runs are presented in the right-hand side of Table I. For the global initiator concentration 0.01*M*, most of the plots of conversion vs. time are represented in Figures 1, 3, and 4. In Figures 1 and 2, the high-temperature and bifunctional initiator

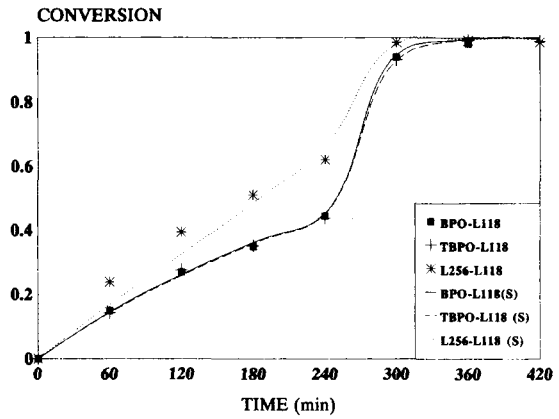

Figure 1 Evolution of conversion, for different mixtures of the investigated low-temperature initiators with the high-temperature and bifunctional initiator L-118. The global initiator concentration was 0.01*M*.

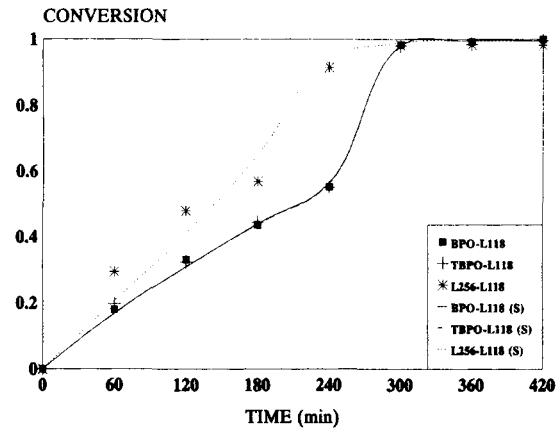

Figure 2 Evolution of conversion, for different mixtures of the investigated low-temperature initiators with the high-temperature and bifunctional initiator L-118. The global initiator concentration was 0.016*M*.

L118 is combined with all the low-temperature initiators at concentration of 0.01*M* and 0.016*M*, respectively. In Figure 3, the low-temperature and monofunctional initiator TBPO is combined with all the high-temperature initiators. In Figure 4, the low-temperature bifunctional initiator L256 is combined with the high-temperature bifunctional initiators. In all figures, the points indicate experimental measurements and the curves represent the model predictions.

THE MODEL ADJUSTMENT

The nomenclature, the kinetic scheme, and the mathematical model were based on Villalobos et al.[5]

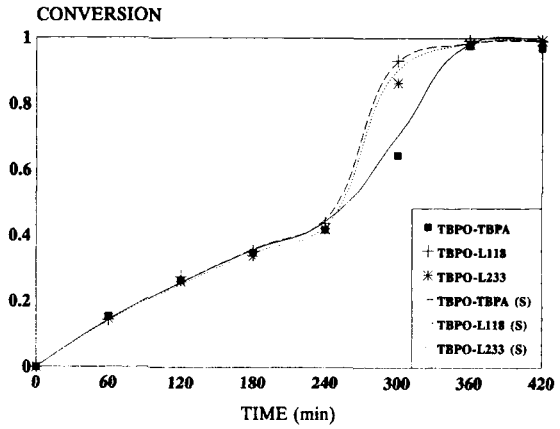

Figure 3 Evolution of conversion, for different mixtures of the low-temperature and monofunctional initiator TBPO with each of the investigated high-temperature initiators.The global initiator concentration was 0.01*M*.

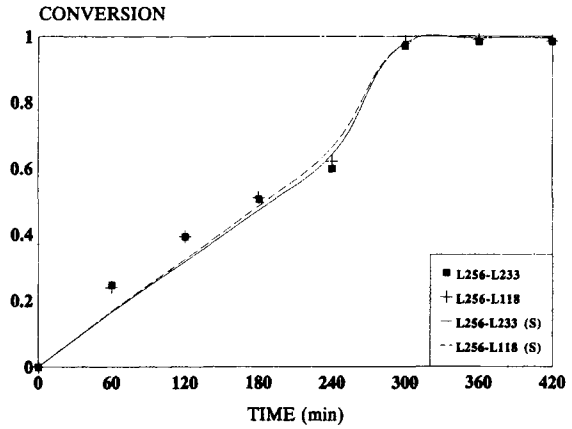

Figure 4 Evolution of conversion, for different mixtures of the low-temperature and bifunctional initiator L256 with the high-temperature and bifunctional initiators. The global initiator concentration was 0.01*M*.

The kinetic scheme of Villalobos et al.[5] was modified (Table II) to admit the use of bi- and/or monofunctional initiator mixtures. From the kinetics of Table II, the mathematical model of the Appendix was developed. The model is able of predicting the time evolution of conversion and of the average molecular weights $\bar{M}_n$ and $\bar{M}_w$.

Most of the kinetic constants were directly adopted from the literature, as shown in Table III. The remaining parameters were set as follows: (a) following Yoon and Choi,[6] the global initiator efficiency (f) was first adjusted to optimally fit the conversion vs. time curves for each of the experimental runs; and (b) the Arrhenius expression for the transfer to the monomer constant (K_{tfm}) was then adjusted to fit the complete set of molecular weight measurements. The procedure is noniterative because K_{tfm} has only a very slight effect on conversion. (The transfer reactions do not affect the number of free radicals.)

A empirical correlation proposed by Hamielec[13] was applied to model the diffusion controled termination reactions at high conversion. Also, propagation rate controled by diffusion was modeled as Villalobos et al.[5]

Consider the adjustment of f. To find the optimal fit of the conversion curves, the Golden[14] optimization method was utilized. The resulting efficiencies are presented in the last column of Table I. The following can be noted: (a) for the high global initiator concentration, lower values of f are observed; and (b) when using bifunctional initiators, the efficiencies were higher than for mixtures of monofunctional initiators.

The decrease in f for higher initiator concentrations is in accord with the results byYoon and Choi[6] for symmetrical bifunctional initiators, and by Kim et al.[15] for a nonsymmetrical bifunctional initiators. The same effect was found by Heffelfinger and Langsam[16] for the copolymerization of vinyl acetate and vinyl chloride with terbutyl perneodecanoate as initiator. For the initiators under study, a possible explanation to the decrease in f follows. The initiators under study may suffer a decarboxilation:

$$R-\overset{\overset{O}{\|}}{C}-O^{\bullet} \rightarrow R^{\bullet} + CO_2$$

followed by a recombination of the R$^{\bullet}$ radicals to generate an inactive molecule. According to ref. 10, the constant of such recombination reaction is in the order of 10^7 L/mol s; while the mean times of neighboring free radicals is between 10^{-10} and 10^{-9} s. Increasing the initiator concentration, the probability of occurrence of the said reactions increases; thus decreasing the initiator efficiency.

Consider now the adjustment of the transfer constant. For the molecular weight measurements of Table I, the best fit resulted: $K_{tfm} = 1.8 \times 10^8 \exp(-12000/RT)$ (L/mol min). This expression is similar to others reported in the literature,[4,6] but differs quite substantially from that in Villalobos et al.[5]

RESULTS AND DISCUSSION

The Conversion Plots

An acceptable fit between the measured and predicted values of conversion can be observed in Figure 1–4. With reference to Figures 1 and 2, the following can be mentioned:

1. In spite of their quite different structural differences, BPO and TBPO both exhibit similar decomposition characteristics, and this is reflected in their practically coincident conversion curves.
2. As expected, the bifunctional initiator L256 presents a higher reaction rate, due to its higher net concentration of peroxide groups. After 3 h of reaction (and at around 60% conversion), the slope of the conversion curve is higher than in the other cases. This is probably due to the combined effects of reinitiation and autoacceleration.[4] Studying the L256 initiator, Villalobos et al.[5] found two

Table II The Adopted Kinetic Mechanism

Initiation Sytem Monofunctional-Monofunctional	Initiation System Monofunctional-Bifunctional	Initiation System Bifunctional-Bifunctional	
Thermal Initiation:			
	$3M \xrightarrow{K_{th}} 2R_I^{\bullet}$		
Chemical Initiation:			
$I_1 \xrightarrow{K_{d_1}} R_{in}^{\bullet} + R_{in}^{\bullet}$	$I_1 \xrightarrow{K_{d_1}} R_{in}^{\bullet} + \tilde{R}_{in}^{\bullet}$	$I_1 \xrightarrow{K_{d_1}} R_{in}^{\bullet} + \tilde{R}_{1,in}^{\bullet}$	$\tilde{P}_{2,r} \xrightarrow{K_{d_2}} R_{in}^{\bullet} + R_r^{\bullet}$ $(r \geq 2)$
$I_2 \xrightarrow{K_{d_2}} R_{in}^{\bullet} + R_{in}^{\bullet}$	$I_2 \xrightarrow{K_{d_2}} R_{in}^{\bullet} + R_{in}^{\bullet}$	$I_2 \xrightarrow{K_{d_2}} R_{in}^{\bullet} + \tilde{R}_{2,in}^{\bullet}$	$\tilde{\tilde{P}}_{1,2,r} \xrightarrow{K_{d_1}} R_{in}^{\bullet} + \tilde{R}_{2,r}^{\bullet}$ $(r \geq 2)$
$R_{in}^{\bullet} + M \xrightarrow{K_1} R_1^{\bullet}$	$R_{in}^{\bullet} + M \xrightarrow{K_1} R_1^{\bullet}$	$R_{in}^{\bullet} + M \xrightarrow{K_1} R_1^{\bullet}$	$\tilde{\tilde{P}}_{1,2,r} \xrightarrow{K_{d_2}} R_{in}^{\bullet} + \tilde{R}1,r$ $(r \geq 2)$
	$\tilde{R}_{in}^{\bullet} + M \xrightarrow{K_2} \tilde{R}_1^{\bullet}$	$\tilde{R}_{1in}^{\bullet} + M \xrightarrow{K_1} \tilde{R}_{1,1}^{\bullet}$	
			$\tilde{\tilde{P}}_{2,2,r} \xrightarrow{K_{d_2}} R_{in}^{\bullet} + \tilde{R}_{2,r}^{\bullet}$ $(r \geq 2)$
	$\tilde{P}_r \xrightarrow{K_{d_2}} R_{in}^{\bullet} + R_r^{\bullet}$ $(r \geq 2)$	$\tilde{R}_{2in}^{\bullet} + M \xrightarrow{K_2} \tilde{R}_{2,1}^{\bullet}$	
			$\tilde{\tilde{P}}_{1,1,r} \xrightarrow{K_{d_1}} R_{in}^{\bullet} + \tilde{R}_{1,r}^{\bullet}$ $(r \geq 2)$
	$\tilde{\tilde{P}}_r \xrightarrow{K_{d_2}} R_{in}^{\bullet} + \tilde{R}_r^{\bullet}$ $(r \geq 2)$	$\tilde{P}_{1,r} \xrightarrow{K_{d_1}} R_{in}^{\bullet} + R_r^{\bullet}$ $(r \geq 2)$	
			$\tilde{R}_{1,r}^{\bullet} + \tilde{R}_{1,s}^{\bullet} \xrightarrow{K_t} \tilde{\tilde{P}}_{1,1,r+s}$
			$\tilde{R}_{1,r}^{\bullet} + \tilde{R}_{2,s}^{\bullet} \xrightarrow{K_t} \tilde{\tilde{P}}_{1,2,r+s}$
			$\tilde{R}_{2,r}^{\bullet} + \tilde{R}_{2,s}^{\bullet} \xrightarrow{K_t} \tilde{\tilde{P}}_{2,2,r+s}$
Transfer to monomer: $(r \geq 1)$			
$R_r^{\bullet} + M \xrightarrow{K_{tfm}} P_r + R_1^{\bullet}$	$R_r^{\bullet} + M \xrightarrow{K_{tfm}} P_r + R_1^{\bullet}$	$R_r^{\bullet} + M \xrightarrow{K_{tfm}} P_r + R_I^{\bullet}$	
	$\tilde{R}_r^{\bullet} + M \xrightarrow{K_{tfm}} \tilde{P}_r + R_1^{\bullet}$	$\tilde{R}_{1,r}^{\bullet} + M \xrightarrow{K_{tfm}} \tilde{P}_{1,r} + R_I^{\bullet}$	
		$\tilde{R}_{2,r}^{\bullet} + M \xrightarrow{K_{tfm}} \tilde{P}_{2,r} + R_I^{\bullet}$	
Propagation: $(r \geq 1)$			
$R_r^{\bullet} + M \xrightarrow{K_p} R_{r+1}^{\bullet}$	$R_r^{\bullet} + M \xrightarrow{K_p} R_{r+1}^{\bullet}$	$R_r^{\bullet} + M \xrightarrow{K_p} R_{r+1}^{\bullet}$	
	$\tilde{R}_r^{\bullet} + M \xrightarrow{K_p} \tilde{R}_{r+1}^{\bullet}$	$\tilde{R}_{1,r}^{\bullet} + M \xrightarrow{K_p} \tilde{R}_{1,r+1}^{\bullet}$	
		$\tilde{R}_{2,r}^{\bullet} + M \xrightarrow{K_p} \tilde{R}_{2,r+1}^{\bullet}$	
Termination: $(r, s \geq 1)$			
$R_r^{\bullet} + R_s^{\bullet} \xrightarrow{K_t} P_{r+s}$	$R_r^{\bullet} + R_s^{\bullet} \xrightarrow{K_t} P_{r+s}$	$R_r^{\bullet} + R_s^{\bullet} \xrightarrow{K_t} P_{r+s}$	
	$R_r^{\bullet} + \tilde{R}_s^{\bullet} \xrightarrow{K_t} \tilde{P}_{r+s}$	$\tilde{R}_{1,r}^{\bullet} + R_s^{\bullet} \xrightarrow{K_t} \tilde{P}_{1,r+s}$	
	$\tilde{R}_r^{\bullet} + \tilde{R}_s^{\bullet} \xrightarrow{K_t} \tilde{\tilde{P}}_{r+s}$	$\tilde{R}_{2,r}^{\bullet} + R_s^{\bullet} \xrightarrow{K_t} \tilde{P}_{2,r+s}$	

different slopes in the curve conversion vs. time (at low and intermediate conversions); explaining this behavior by the sequential decomposition of the peroxide groups.

With reference to Figures 3 and 4, note the following:

1. The effect of high-temperature initiators is less pronounced than in Figure 1.
2. The bifunctional initiators again provide the highest reaction rates. The efficiency of such initiators seems to depend on the monomer concentration. When biperoxides were used for both the low- and the high-temperature initiators, the effect of the second proved relatively moderate. This is due to the high rates of polymerization at low reaction times produced by the low-temperature bifunctional initiator.

The Molecular Weights

Consider now the average molecular weights presented in the right-hand side of Table I. The following can be observed:

1. As expected, the molecular weights decrease as the global initiator concentration change

Table III The Adopted Kinetic Constants

	$K_{TH} = 1.314 \times 10^7 \exp(-27440/RT)$	$L^2\ mol^{-2}\ min^{-1}$	Ref. 6
	$K_p = 6.126 \times 10^8 \exp(-7067/RT)$	$L\ mol^{-1}\ min^{-1}$	Ref. 5
	$K_{tc} = 1.000 \times 10^{11} \exp(-1677.8/RT)$	$L\ mol^{-1}\ min^{-1}$	Ref. 5
BPO	$K_d = 7.409 \times 10^{16} \exp(-31360.7/RT)$	min^{-1}	[a]
TBPO	$K_d = 5.478 \times 10^{15} \exp(-29508.2/RT)$	min^{-1}	[a]
TBPA	$K_d = 6.134 \times 10^{17} \exp(-35467.2/RT)$	min^{-1}	[a]
L256	$K_d = 1.251 \times 10^{17} \exp(-31700/RT)$	min^{-1}	[a]
L118	$K_d = 3.337 \times 10^{18} \exp(-37145.2/RT)$	min^{-1}	[a]
L233-M75	$K_d = 2.251 \times 10^{17} \exp(-36555.6/RT)$	min^{-1}	[a]

[a] Technical data. Pennwalt Lucidol (1980).

from 0.01 to 0.016 M. This is a consequence of the increased rate of termination at a higher free radical concentration.

2. Compare the average molecular weights produced with the low-temperature initiators TBPO and L256. While the $\bar{M}_n$s produced with the first initiator are slightly higher than those produced with the second, the opposite is verified with the corresponding $\bar{M}_w$s. The higher polydispersities of bifunctional initiators with respect to monofunctional are in accord with the results by Villalobos et al.,[5] and may be explained by the reinitiation reactions that occur when bifunctional initiators with peroxide groups of different thermal stabilities are utilized.
3. Compare the results with BPO and TBPO for a given global concentration. Although both polymerization rates are similar, the average molecular weights obtained with BPO are lower than with TBPO. This may be indicative of transfer reactions associated to the former initiator. (From the characterization—by UV spectrometry—of PS obtained with BPO, García and Patel[17] detected the presence of more than one terminal group per polymer molecule, thus indicating transfer reactions and/or induced decomposition reactions.)
4. In spite of the fact that the decomposition caracteristics of TBPA are similar to those of L118, the average molecular weights of the polymers produced with both initiators are also quite similar. This could be explained by the fact that transfer reactions associated to the L118 radicals may be reducing the final molecular weights, thus compensating reinitiation. (The transfer reactions assumption is supported by the fact that the radicals generated from the L118 initiator are identical to those generated from BPO.)
5. The molecular weights obtained with the L233-M75 initiator were lower than with the other bifunctional initiators due to the higher decomposition temperature of the former. This explains the change in polydispersity that tends to decrease with increasing temperatures.[4]
6. Discrepancies as high as 50% between measured and predicted values of the average molecular weight are observed. However, more than half of the predictions are within 15% of the corresponding measurements. The discrepancies may be due to measurement errors, and to the simplifications in the kinetic scheme such as: (a) assigning identical thermal stabilities to the different peroxide groups, (b) equal efficiency values for both initiators (low and high temperature), and (c) not considering reactions such as the chain transfers to the initiator and to the polymer.

CONCLUSIONS

In the bulk polymerization of S, the use of initiator mixtures that include bifunctional initiators seems beneficial to reduce reaction times, while maintaining and even improving polymer quality. The previous conclusion may be inferred from the following experimental observations:

1. In combination with a high-temperature initiator, and for equal concentrations, the low-temperature and bifunctional initiator L256 noticeably increases polymerization rate with respect to the low-temperature (but monofunctional) initiators BPO and TBPO. Also, the L256 initiator increases $\bar{M}_w$ and the polydispersity.

2. In combination with a low-temperature initiator and for equal concentrations, the other investigated bifunctional initiators (L118 and L233-M75) showed reduced benefits on polymerization rate with respect to TBPA. With L118, the molecular weights remained practically unmodified; and with L233-M75, the molecular weights were even lower than with TBPA. This is possibly due to the relatively higher decomposition temperature of L233-M75.

The mathematical model adequately reproduced the conversion curves, while larger deviations were observed for the molecular weight averages. However, it should be borne in mind that while the efficiency was adjusted for every experimental run, a single expression for the transfer coefficient was used to fit the complete set of molecular weight measurements. The model confirmed previous publications in the sense that the global initiator efficiency seems to decrease with increasing initiator concentrations.

Thanks to CONDES (Universidad del Zulia, Venezuela) for their financial support, INDESCA for determinations of MWD, and Estirenos del Zulia for their gifts of the samples.

APPENDIX

Kinetic Equations for the Bifunctional–Bifunctional Initiation System

The kinetic equations for each species in styrene polymerization with mixtures of bifunctional initiators are developed from the proposed reaction mechanism as follows.

For a Batch Reactor

Primary radicals balance:

$$\frac{1}{V}\frac{d([R_{in}^{\bullet}]V)}{dt} = fKd_1[I_1] + fKd_2[I_2] + fKd_1([\tilde{P}_{1,r}] + [\tilde{\tilde{P}}_{1,2,r}] + [\tilde{\tilde{P}}_{1,1,r}]) + fKd_2([\tilde{P}_{2,r}] + [\tilde{\tilde{P}}_{1,2,r}] + [\tilde{\tilde{P}}_{2,2,r}]) - K_1[M][R_{in}^{\bullet}] \quad (1)$$

$$\frac{1}{V}\frac{d([\tilde{R}_{1,in}^{\bullet}]V)}{dt} = fKd_1[I_1] - K_2[M][\tilde{R}_{1,in}^{\bullet}] \quad (2)$$

$$\frac{1}{V}\frac{d([\tilde{R}_{2,in}^{\bullet}]V)}{dt} = fKd_2[I_2] - K_3[M][\tilde{R}_{2,in}^{\bullet}]. \quad (3)$$

The efficiency (f), it is assumed constant through the polymerization and the same for both initiators and for macroinitiator molecules ($\tilde{P}_r$, $\tilde{\tilde{P}}_{z,k,r}$).

Applying the steady-state hypothesis for radical concentrations:

$$[R_{in}^{\bullet}] = \frac{fKd_1[I_1] + fKd_2[I_2] + fKd_1([\tilde{P}_{1,r}] + [\tilde{\tilde{P}}_{1,2,r}] + [\tilde{\tilde{P}}_{1,1,r}]) + fKd_2([\tilde{P}_{2,r}] + [\tilde{\tilde{P}}_{1,2,r}[+ [\tilde{\tilde{P}}_{2,2,r}])}{K_1[M]} \quad (4)$$

$$[\tilde{R}_{1,in}^{\bullet}] = \frac{fKd_1[I_1]}{K_2[M]} \quad (5)$$

$$[\tilde{R}_{2,in}^{\bullet}] = \frac{fKd_2[I_2]}{K_3[M]}. \quad (6)$$

For thermal initiation:

$$R_{th} = 2K_{th}[M]^3 \quad (7)$$

The initiation rates for radicals with and without peroxide groups can be expressed as:

$$R_{IN} = K_1[M][R_{in}^{\bullet}] \quad (8)$$

$$\tilde{R}_{1,IN} = K_2[M][\tilde{R}_{1,in}^{\bullet}] \quad (9)$$

$$\tilde{R}_{2,IN} = K_3[M][\tilde{R}_{2,in}^{\bullet}]. \quad (10)$$

Replacing eqs. (4), (5), and (6) into eqs. (8), (9), and (10), respectively, one obtains:

$$R_{IN} = fKd_1[I_1] + fKd_2[I_2] + fKd_1([\tilde{P}_{1,r}] + [\tilde{\tilde{P}}_{1,2,r}] + [\tilde{\tilde{P}}_{1,1,r}]) + fKd_2([\tilde{P}_{2,r}] + [\tilde{\tilde{P}}_{1,2,r}] + [\tilde{\tilde{P}}_{2,2,r}]) \quad (11)$$

$$\tilde{R}_{1,IN} = fKd_1[I_1] \quad (12)$$

$$\tilde{R}_{2,IN} = fKd_2[I_2]. \quad (13)$$

For growing radicals:

The total concentration of radical species with and without undecomposed peroxide groups is defined as:

$$y_{TO} = [R_r^{\bullet}] + [\tilde{R}_{1,r}^{\bullet}] + [\tilde{R}_{2,r}^{\bullet}] \quad (14)$$

$$\frac{1}{V}\frac{d([R_I^{\bullet}]V)}{dt} = R_{IN} - K_p[R_I^{\bullet}][M] - K_t[R_I^{\bullet}]y_{TO} + K_{tfm}[M]y_{TO} - K_{tfm}[R_I^{\bullet}][M] + R_{th} \quad (15)$$

$$\frac{1}{V}\frac{d([R_r^\bullet]V)}{dt} = fKd_1[\tilde{P}_{1,r}] + fKd_2[\tilde{P}_{2,r}] + K_p[M]([R_{r-1}^\bullet] - [R_r^\bullet]) - K_{tfm}[R_r^\bullet][M] - K_t[R_r^\bullet]Y_{to} \quad (16)$$

$$\frac{1}{V}\frac{d([\tilde{R}_{1,1}^\bullet]V)}{dt} = K_2[\tilde{R}_{1,in}][M] - K_p[\tilde{R}_{1,1}^\bullet][M] - K_t[\tilde{R}_{1,1}^\bullet]Y_{to} - K_{tfm}[\tilde{R}_{1,1}^\bullet][M] \quad (17)$$

$$\frac{1}{V}\frac{d([\tilde{R}_{1,r}^\bullet]V)}{dt} = fKd_2[\tilde{\tilde{P}}_{1,2,r}] + fKd_1[\tilde{\tilde{P}}_{1,1,r}] - K_p[\tilde{R}_{1,r}^\bullet][M] + K_p[\tilde{R}_{1,r-1}^\bullet][M] - K_t[\tilde{R}_{1,r}^\bullet][R_s^\bullet] - K_t[\tilde{R}_{1,r}^\bullet][\tilde{R}_{1,s}^\bullet] - K_t[\tilde{R}_{1,r}^\bullet][\tilde{R}_{2,s}^\bullet] - K_{tfm}[\tilde{R}_{1,r}^\bullet][M] \quad (18)$$

$$\frac{1}{V}\frac{d([\tilde{R}_{2,1}^\bullet]V)}{dt} = K_3[\tilde{R}_{2,in}][M] - K_p[\tilde{R}_{2,1}^\bullet][M] - K_t[\tilde{R}_{2,1}^\bullet]Y_{to} - K_{tfm}\tilde{R}_{2,1}^\bullet][M] \quad (19)$$

$$\frac{1}{V}\frac{d([\tilde{R}_{2,r}^\bullet]V)}{dt} = fKd_1[\tilde{\tilde{P}}_{1,2,r}] + fKd_2[\tilde{\tilde{P}}_{2,2,r}] - K_p[\tilde{R}_{2,r}^\bullet][M] + K_p[\tilde{R}_{2,r-1}^\bullet][M] - K_t[\tilde{R}_{2,r}^\bullet][R_s^\bullet] - K_t[\tilde{R}_{2,r}^\bullet][\tilde{R}_{1,s}^\bullet] - K_t[\tilde{R}_{2,r}^\bullet][\tilde{R}_{2,s}^\bullet] - K_{tfm}[\tilde{R}_{2,r}^\bullet][M]. \quad (20)$$

Polymer Species Balance

$$\frac{1}{V}\frac{d([P_r]V)}{dt} = K_{tfm}[R_r^\bullet][M] + \frac{1}{2}K_t\sum_{s=1}^{r-1}[R_{r-s}^\bullet][R_s^\bullet] \quad (21)$$

$$\frac{1}{V}\frac{d([\tilde{P}_{1,r}]V)}{dt} = -Kd_1[\tilde{P}_{1,r}] + K_t\sum_{s=1}^{r-1}[\tilde{R}_{1,r-s}^\bullet][R_s^\bullet] + K_{tfm}[\tilde{R}_{1,r}^\bullet][M] \quad (22)$$

$$\frac{1}{V}\frac{d([\tilde{P}_{2,r}]V)}{dt} = Kd_2[\tilde{P}_{2,r}] + K_t\sum_{s=1}^{r-1}[\tilde{R}_{2,r-s}^\bullet][R_s^\bullet] + K_{tfm}[\tilde{R}_{2,r}^\bullet][M] \quad (23)$$

$$\frac{1}{V}\frac{d([\tilde{\tilde{P}}_{1,1,r}]V)}{dt} = -Kd_1[\tilde{\tilde{P}}_{1,1,r}] + \frac{1}{2}K_t\sum_{s=1}^{r-1}[\tilde{R}_{1,r-s}^\bullet][\tilde{R}_{1,s}^\bullet] \quad (24)$$

$$\frac{1}{V}\frac{d([\tilde{\tilde{P}}_{1,2,r}]V)}{dt} = -(Kd_1 + Kd_2)[\tilde{\tilde{P}}_{1,2,r}] + K_t\sum_{s=1}^{r-1}[\tilde{R}_{1,r-s}^\bullet][\tilde{R}_{2,s}^\bullet] \quad (25)$$

$$\frac{1}{V}\frac{d([\tilde{\tilde{P}}_{2,2,r}]V)}{dt} = -Kd_2[\tilde{\tilde{P}}_{2,2,r}] + \frac{1}{2}K_t\sum_{s=1}^{r-1}[\tilde{R}_{2,r-s}^\bullet][\tilde{R}_{2,s}^\bullet]. \quad (26)$$

Monomer and Initiators Consumption

Monomer consumption through initiation thermal and chemical and transfer to monomer is neglected. Then, the following balance for monomer applies for a batch reactor:

$$\frac{1}{V}\frac{dN_M}{dt} = -K_pY_{to}[M]. \quad (27)$$

The bifunctional initiators is only consumed by its homolytic decomposition, its balance resulting:

$$\frac{1}{V}\frac{dN_{I_1}}{dt} = -Kd_1[I_1] \quad (28)$$

$$\frac{1}{V}\frac{dN_{I_2}}{dt} = -Kd_2[I_2]. \quad (29)$$

Conversion and Number Average and Weight Average Molecular Weight

The ith-moment for the concentration distributions of polymeric species and radicals are defined as:

$$Q_i = \sum_{r=1}^{\infty} r^j[P_r] \quad \text{dead polymer}$$

$$\left.\begin{aligned}\tilde{Q}_i &= \sum_{r=1}^{\infty} r^j[\tilde{P}_r]\\ \tilde{\tilde{Q}}_i &= \sum_{r=1}^{\infty} r^j[\tilde{\tilde{P}}_r]\end{aligned}\right\} \quad \text{temporally dead polymer}$$

$$\left.\begin{aligned}Y_i &= \sum_{r=1}^{\infty} r^i[R_r]\\ \tilde{Y}_i &= \sum_{r=1}^{\infty} r^i[\tilde{R}_r]\end{aligned}\right\} \quad \text{live polymer}$$

The differential equations representing the variation with respect to time of the moments of the radical and polymer concentration distributions are described for the bifunctional-bifunctional initiation system as:

For Radicals:

Zeroeth Moment:

$$\frac{1}{V}\frac{d([y_o]V)}{dt} = R_{IN} + fKd_1\tilde{Q}_{1,0} + fKd_2\tilde{Q}_{2,0} - K_t y_{to} y_0 + K_{tfm}[M](\tilde{y}_{1,0} + \tilde{y}_{2,0}) \quad (30)$$

$$\frac{1}{V}\frac{d([\tilde{y}_{1,0}]V)}{dt} = \tilde{R}_{1,IN} + fKd_2\tilde{\tilde{Q}}_{1,2,0} + fKd_1\tilde{\tilde{Q}}_{1,1,0} - K_t\tilde{y}_{1,0}y_{to} - K_{tfm}[M]\tilde{y}_{1,0} \quad (31)$$

$$\frac{1}{V}\frac{d([\tilde{y}_{2,0}]V)}{dt} = \tilde{R}_{2,IN} + fKd_1\tilde{\tilde{Q}}_{1,2,0} + fKd_2\tilde{\tilde{Q}}_{2,2,0} - K_t\tilde{y}_{2,0}y_{to} - K_{tfm}[M]\tilde{y}_{2,0} \quad (32)$$

First Moment:

$$\frac{1}{V}\frac{d([y_1]V)}{dt} = R_{IN} + fKd_1\tilde{Q}_{1,1} + fKd_2\tilde{Q}_{2,1} + K_p[M]y_0 - K_t y_{to} y_1 + K_{tfm}[M](y_{to} - y_1) \quad (33)$$

$$\frac{1}{V}\frac{d([\tilde{y}_{1,1}]V)}{dt} = \tilde{R}_{1,IN} + fKd_2\tilde{\tilde{Q}}_{1,2,1} + fKd_1\tilde{\tilde{Q}}_{1,1,1} + K_p[M]\tilde{y}_{1,0} - K_t y_{to}\tilde{y}_{1,1} - K_{tfm}[M]\tilde{y}_{1,1} \quad (34)$$

$$\frac{1}{V}\frac{d([\tilde{y}_{2,1}]V)}{dt} = \tilde{R}_{2,IN} + fKd_1\tilde{\tilde{Q}}_{1,2,1} + fKd_2\tilde{\tilde{Q}}_{2,2,1} + K_p[M]\tilde{y}_{2,0} - K_t y_{to}\tilde{y}_{2,1} - K_{tfm}[M]\tilde{y}_{2,1} \quad (35)$$

Second Moment:

$$\frac{1}{V}\frac{d([y_2]V)}{dt} = R_{IN} + fKd_1\tilde{Q}_{1,2} + fKd_2\tilde{Q}_{2,2} + K_p[M](y_0 + 2y_1) - K_t y_{to} y_2 + K_{tfm}[M](y_{to} - y_2) \quad (36)$$

$$\frac{1}{V}\frac{d([\tilde{y}_{1,2}]V)}{dt} = \tilde{R}_{1,IN} + fKd_2\tilde{\tilde{Q}}_{1,2,2} + fKd_1\tilde{\tilde{Q}}_{1,1,2} + K_p[M](\tilde{y}_{1,0} + 2\tilde{y}_{1,1}) - K_t y_{to}\tilde{y}_{1,2} - K_{tfm}[M]\tilde{y}_{1,2} \quad (37)$$

$$\frac{1}{V}\frac{d([\tilde{y}_{2,2}]V)}{dt} = \tilde{R}_{2,IN} + fKd_1\tilde{\tilde{Q}}_{1,2,2} + fKd_2\tilde{\tilde{Q}}_{2,2,2} + K_p[M](\tilde{y}_{2,0} + 2\tilde{y}_{2,1}) - K_t y_{to}\tilde{y}_{2,2} - K_{tfm}[M]\tilde{y}_{2,2} \quad (38)$$

The eqs. (30)-(38) can be simplified to a set of algebraic equations applying the steady-state hypothesis for radical concentration and assuming $y_2 \gg y_1 \gg y_0$ for both types of radicals.

$$y_0 = \frac{R_{IN} + fKd_1\tilde{Q}_{1,0} + fKd_2\tilde{Q}_{2,0} + K_{tfm}[M](\tilde{y}_{1,0} + \tilde{y}_{2,0})}{K_t y_{to}} \quad (39)$$

$$\tilde{y}_{1,0} = \frac{\tilde{R}_{1,IN} + fKd_2\tilde{\tilde{Q}}_{1,2,0} + fKd_1\tilde{\tilde{Q}}_{1,1,0}}{K_t y_{to} + K_{tfm}[M]} \quad (40)$$

$$\tilde{y}_{2,0} = \frac{\tilde{R}_{2,IN} + fKd_1\tilde{\tilde{Q}}_{1,2,0} + fKd_2\tilde{\tilde{Q}}_{2,2,0}}{K_t y_{to} + K_{tfm}[M]} \quad (41)$$

$$y_1 = \frac{R_{IN} + fKd_1\tilde{Q}_{1,1} + fKd_2Q_{2,1} + Kp[M]y_0}{K_t y_{to} + K_{tfm}[M]} \quad (42)$$

$$\tilde{y}_{1,1} = \frac{\tilde{R}_{1,IN} + fKd_2\tilde{\tilde{Q}}_{1,2,1} + fKd_1\tilde{\tilde{Q}}_{1,1,1} + Kp[M]\tilde{y}_{1,0}}{K_t y_{to} + K_{tfm}[M]} \quad (43)$$

$$\tilde{y}_{2,1} = \frac{\tilde{R}_{2,IN} + fKd_1\tilde{\tilde{Q}}_{1,2,1} + fKd_2\tilde{\tilde{Q}}_{2,2,1} + Kp[M]\tilde{y}_{2,0}}{K_t y_{to} + K_{tfm}[M]} \quad (44)$$

$$y_2 = \frac{R_{IN} + fKd_1\tilde{Q}_{1,2} + fKd_2\tilde{Q}_{2,2} + 2Kp[M]y_1}{K_t y_{to} + K_{tfm}[M]} \quad (45)$$

$$\tilde{y}_{1,2} = \frac{\tilde{R}_{1,IN} + fKd_2\tilde{\tilde{Q}}_{1,2,2} + fKd_1\tilde{\tilde{Q}}_{1,1,2} + Kp[M](2\tilde{y}_{1,1} + \tilde{y}_{1,0})}{K_t\tilde{y}_{1,2} + K_{tfm}[M]} \quad (46)$$

$$\tilde{y}_{2,2} = \frac{\tilde{R}_{2,IN} + fKd_1\tilde{\tilde{Q}}_{1,2,2} + fKd_2\tilde{\tilde{Q}}_{2,2,2} + Kp[M](2\tilde{y}_{2,1} + \tilde{y}_{2,0})}{K_t y_{to} + K_{tfm}[M]} \quad (47)$$

For Polymeric Species:

Zeroeth Moment:

$$\frac{1}{V}\frac{d([Q_0]V)}{dt} = K_{tfm}[M]y_0 + \frac{1}{2}K_t y_0^2 \quad (48)$$

$$\frac{1}{V}\frac{d([\tilde{Q}_{1,0}]V)}{dt} = -Kd_1\tilde{Q}_{1,0} + K_t\tilde{y}_{1,0}y_0 + K_{tfm}[M]\tilde{y}_{1,0} \quad (49)$$

$$\frac{1}{V}\frac{d([\tilde{Q}_{2,0}]V)}{dt} = -Kd_2\tilde{Q}_{2,0} + \mathrm{K}_t\tilde{y}_{2,0}y_0 + K_{tfm}[M]\tilde{y}_{2,0} \quad (50)$$

$$\frac{1}{V}\frac{d([\tilde{\tilde{Q}}_{1,1,0}]V)}{dt} = -Kd_1\tilde{\tilde{Q}}_{1,1,0} + \frac{1}{2}K_t\tilde{y}_{1,0}^2 \quad (51)$$

$$\frac{1}{V}\frac{d([\tilde{\tilde{Q}}_{1,2,0}]V)}{dt} = -(Kd_1 + Kd_2)\tilde{\tilde{Q}}_{1,2,0} + K_t\tilde{y}_{1,0}\tilde{y}_{2,0} \quad (52)$$

$$\frac{1}{V}\frac{d([\tilde{\tilde{Q}}_{2,2,0}]V)}{dt} = -Kd_2\tilde{\tilde{Q}}_{2,2,0} + \frac{1}{2}K_t\tilde{y}_{2,0}^2 \quad (53)$$

First Moment:

$$\frac{1}{V}\frac{d([Q_1]V)}{dt} = K_{tfm}[M]y_1 + K_t y_1 y_0 \quad (54)$$

$$\frac{1}{V}\frac{d([\tilde{Q}_{1,1}]V)}{dt} = -Kd_1\tilde{Q}_{1,1} + \mathrm{K}_t(\tilde{y}_{1,0}y_1 + \tilde{y}_{1,1}y_0) + K_{tfm}[M]\tilde{y}_{1,1} \quad (55)$$

$$\frac{1}{V}\frac{d([\tilde{Q}_{2,1}[V)}{dt} = -Kd_2\tilde{Q}_{2,1} + \mathrm{K}_t(\tilde{y}_{2,1}y_0 + \tilde{y}_{2,0}y_1) + K_{tfm}[M]\tilde{y}_{2,1} \quad (56)$$

$$\frac{1}{V}\frac{d([\tilde{\tilde{Q}}_{1,1,1}]V)}{dt} = -Kd_1\tilde{\tilde{Q}}_{1,1,1} + K_t\tilde{y}_{1,0}\tilde{y}_{1,1} \quad (57)$$

$$\frac{1}{V}\frac{d([\tilde{\tilde{Q}}_{2,2,1}]V)}{dt} = -Kd_2\tilde{\tilde{Q}}_{2,2,1} + K_t\tilde{y}_{2,0}\tilde{y}_{2,1} \quad (58)$$

$$\frac{1}{V}\frac{d([\tilde{\tilde{Q}}_{1,2,1}]V)}{dt} = -(Kd_1 + Kd_2)\tilde{\tilde{Q}}_{1,2,1} + \mathrm{K}_t(\tilde{y}_{1,1}\tilde{y}_{2,0} + \tilde{y}_{2,1}\tilde{y}_{1,0}) \quad (59)$$

Second Moment:

$$\frac{1}{V}\frac{d([Q_2]V)}{dt} = K_{tfm}[M]y_2 + K_t(y_0y_2 + y_1^2) \quad (60)$$

$$\frac{1}{V}\frac{d([\tilde{Q}_{1,2}]V)}{dt} = -Kd_1\tilde{Q}_{1,2} + K_t(\tilde{y}_{1,0}y_2 + 2y_1\tilde{y}_{1,1} + y_0\tilde{y}_{1,2}) + K_{tfm}[M]\tilde{y}_{1,2} \quad (61)$$

$$\frac{1}{V}\frac{d([\tilde{Q}_{2,2}]V)}{dt} = -Kd_2\tilde{Q}_{2,2} + K_t(\tilde{y}_{2,0}y_2 + 2y_1\tilde{y}_{2,1} + y_0\tilde{y}_{2,2}) + K_{tfm}[M]\tilde{y}_{2,2} \quad (62)$$

$$\frac{1}{V}\frac{d([\tilde{\tilde{Q}}_{1,1,2}]V)}{dt} = -Kd_1\tilde{\tilde{Q}}_{1,1,2} + \mathrm{K}_t(\tilde{y}_{1,1}^2 + \tilde{y}_{1,2}\tilde{y}_{1,0}) \quad (63)$$

$$\frac{1}{V}\frac{d([\tilde{\tilde{Q}}_{2,2,2}]V)}{dt} = -Kd_2\tilde{\tilde{Q}}_{2,2,2} + \mathrm{K}_t(\tilde{y}_{2,1}^2 + \tilde{y}_{2,2}\tilde{y}_{2,0}) \quad (64)$$

$$\frac{1}{V}\frac{d([\tilde{\tilde{Q}}_{1,2,2}]V)}{dt} = -(Kd_1 + Kd_2)\tilde{\tilde{Q}}_{1,2,2} + \mathrm{K}_t(\tilde{y}_{1,2}\tilde{y}_{2,0} + 2\tilde{y}_{2,1}\tilde{y}_{1,1} + \tilde{y}_{1,0}\tilde{y}_{2,2}) \quad (65)$$

From the simultaneous solution of the system of algebraic (39)–(47) equations and differential (48)–(65) equations the conversion and molecular weight averages development with time are calculated as:

$$X_t = \frac{[M]_0 - [M]_t}{[M]_0} \quad (66)$$

$$\overline{Mn}_{(t)} = \frac{Mw_M(Q_{1(t)} + \tilde{Q}_{1,1(t)} + \tilde{Q}_{2,1(t)} + \tilde{\tilde{Q}}_{1,1,1(t)} + \tilde{\tilde{Q}}_{2,2,1(t)} + \tilde{\tilde{Q}}_{1,2,1(t)} + y_{1(t)} + \tilde{y}_{1,1(t)} + \tilde{y}_{2,1(t)})}{(Q_{0(t)} + \tilde{Q}_{1,0(t)} + \tilde{Q}_{2,0(t)} + \tilde{\tilde{Q}}_{1,1,0(t)} + \tilde{\tilde{Q}}_{1,2,0(t)} + \tilde{\tilde{Q}}_{2,2,0(t)} + y_{0(t)} + \tilde{y}_{1,0(t)} + \tilde{y}_{2,0(t)})} \quad (67)$$

$$\overline{Mw}_{(t)} = \frac{Mw_M(Q_{2(t)} + \tilde{Q}_{1,2(t)} + \tilde{Q}_{2,2(t)} + \tilde{\tilde{Q}}_{1,1,2(t)} + \tilde{\tilde{Q}}_{2,2,2(t)} + \tilde{\tilde{Q}}_{1,2,2(t)} + y_{2(t)} + \tilde{y}_{1,2(t)} + \tilde{y}_{2,2(t)})}{(Q_{1(t)} + \tilde{Q}_{1,1(t)} + \tilde{Q}_{2,1(t)} + \tilde{\tilde{Q}}_{1,1,1(t)} + \tilde{\tilde{Q}}_{1,2,1(t)} + \tilde{\tilde{Q}}_{2,2,1(t)} + y_{1(t)} + \tilde{y}_{1,1(t)} + \tilde{y}_{2,1(t)})} \quad (68)$$

Similarly, the algebraic equations for radical concentration and the differential equations representing the variation with respect to time of the moment of the polymer concentration distributions for monofunctional–monofunctional and bifunctional–monofunctional systems, may be written as follows:

Monofunctional–Monofunctional Initiation System

For Radicals and Polymeric Species:

$$y_0 = \left(\frac{R_I}{K_{tc}}\right)^{1/2} \quad (69)$$

$$y_1 = \frac{R_I + K_p[M]y_0}{K_{tc}y_0 + K_{tfm}[M]} \quad (70)$$

$$y_2 = \frac{R_I + 2K_p[M]y_1}{K_{tc}y_0 + K_{tfm}[M]} \quad (71)$$

$$\frac{1}{V}\frac{d([Q_0]V)}{dt} = \frac{1}{2}K_{tc}y_0^2 + K_{tfm}[M]y_0 \quad (72)$$

$$\frac{1}{V}\frac{d([Q_1]V)}{dt} = K_{tc}y_1y_0 + K_{tfm}[M]y_1 \quad (73)$$

$$\frac{1}{V}\frac{d([Q_2]V)}{dt} = -K_{tfm}[M]y_2 + K_{tc}(y_0y_2 + y_1^2) \quad (74)$$

Monofunctional–Bifunctional Initiation System

For Radicals Species:

$$y_0 = \frac{R_I + K_{tfm}[M]\tilde{y}_0 + 2fKd_2\tilde{Q}_0}{K_{tc}y_{to}} \quad (75)$$

$$\tilde{y}_0 = \frac{\tilde{R}_I + 2fKd_2\tilde{\tilde{Q}}_0}{K_{tc}y_{to} + K_{tfm}[M]} \quad (76)$$

$$y_1 = \frac{R_I + 2fKd_2\tilde{Q}_1 + Kp[M]y_0}{K_{tc}y_{to} + K_{tfm}[M]} \quad (77)$$

$$\tilde{y}_1 = \frac{\tilde{R}_I + 2fKd_2\tilde{Q}_1 + Kp[M]\tilde{y}_0}{K_{tc}y_{to} + K_{tfm}[M]} \quad (78)$$

$$y_2 = \frac{R_I + 2fKd_2\tilde{Q}_2 + 2Kp[M]y_1}{K_{tc}y_{to} + K_{tfm}[M]} \quad (79)$$

$$\tilde{y}_2 = \frac{\tilde{R}_I + 2fKd_2\tilde{\tilde{Q}}_2 + 2Kp[M]\tilde{y}_1}{K_{tc}y_{to} + K_{tfm}[M]} \quad (80)$$

For Polymeric Species:

$$\frac{1}{V}\frac{d([Q_0]V)}{dt} = K_{tfm}[M]y_0 + \frac{1}{2}K_{tc}y_0^2 \quad (81)$$

$$\frac{1}{V}\frac{d([\tilde{Q}_0]V)}{dt} = -2Kd_2\tilde{Q}_0 + K_{tc}\tilde{y}_0y_0 + K_{tfm}[M]\tilde{y}_0 \quad (82)$$

$$\frac{1}{V}\frac{d([\tilde{\tilde{Q}}_0]V)}{dt} = -2Kd_2\tilde{\tilde{Q}}_0 + \frac{1}{2}K_{tc}\tilde{y}_0^2 \quad (83)$$

$$\frac{1}{V}\frac{d(Q_1V)}{dt} = K_{tfm}[M]y_1 + K_{tc}y_1y_0 \quad (84)$$

$$\frac{1}{V}\frac{d([\tilde{Q}_1]V)}{dt} = -2Kd_2\tilde{Q}_1 + K_{tc}(\tilde{y}_1y_0 + \tilde{y}_0y_1) + K_{tfm}[M]\tilde{y}_1 \quad (85)$$

$$\frac{1}{V}\frac{d([\tilde{\tilde{Q}}_1]V)}{dt} = -2Kd_2\tilde{\tilde{Q}}_1 + K_{tc}\tilde{y}_1\tilde{y}_0 \quad (86)$$

$$\frac{1}{V}\frac{d([Q_2]V)}{dt} = K_{tfm}[M]_{y2} + K_{tc}(y_0y_2 + y_1^2) \quad (87)$$

$$\frac{1}{V}\frac{d([\tilde{Q}_2]V)}{dt} = -2Kd_2\tilde{Q}_2 + K_{tc}(2\tilde{y}_1y_1 + y_0\tilde{y}_2 + \tilde{y}_0y_2) + K_{tfm}[M]\tilde{y}_2 \quad (88)$$

$$\frac{1}{V}\frac{d([\tilde{\tilde{Q}}_2[V)}{dt} = -2Kd_2\tilde{\tilde{Q}}_2 + K_{tc}(\tilde{y}_1^2 + \tilde{y}_2\tilde{y}_0) \quad (89)$$

NOMENCLATURE

I_n:	initiator molecule monofunctional or bifunctional; n = 1 or 2
$R^{\bullet}_{in}$:	initiator radical
$\tilde{R}^{\bullet}_{in}$:	initiator radical with one undecomposed peroxide
$\tilde{R}^{\bullet}_{z,in}$:	initiator radical with undecomposed peroxides coming from bifunctional initiator Z = 1 or 2
$R^{\bullet}_r (r \geq 1)$:	macroradical with r repetitive units of S.
$\tilde{R}^{\bullet}_{z,r} (r \geq 1)$:	macroradical with undecomposed peroxides coming from bifunctional initiator Z = 1 or 2.
P_r:	dead polymer molecule.
$\tilde{P}_{z,r}$:	dead polymer with one undecomposed peroxide coming from bifunctional initiator Z = 1 or 2.
$\tilde{\tilde{P}}_{z,k,r}$:	dead polymer with two undecomposed peroxides coming from bifunctional initiators Z = 1 or 2 and K = 1 or 2.

REFERENCES

1. J. Squire and G. Gammon, Pat. N 892672 (1972).
2. V. R. Kamath, U.S. Pat. N 4,129,703 (1978).
3. V. R. Kamath, U.S. Pat. N 4,125,695 (1978).
4. K. Y. Choi, W. R. Liang, and G. D. Lei, *J. Appl. Polym. Sci.*, **35**, 1547 (1988).
5. M. A. Villalobos, A. E. Hamielec, and P. E. Wood, *J. Appl. Poly. Sci.*, **42**, 629 (1991).
6. W. J. Yoon and K. Y. Choi, *Polymer*, **33**(21), 4582 (1992).
7. K. F. O'Driscoll and J. C. Bevington, *Eur. Polym. J.*, **21**(12), 1039–1043 (1985).
8. N. V. Akzo, G.B. Pat. 1,366,977 (1974).
9. C. I. Simionescu and A. A. Popa, *Polym. Plast. Technol. Eng.*, **31**, 451–461 (1992).

10. G. Odian, *Principles of Polymerization,* 2nd ed., Wiley Interscience, New York, 1981.
11. S. S. Ivanchev, *Polym. Sci. USSR,* **20,** 2157 (1979).
12. S. I. Kuchanov, N. G. Ivanova, and S. S. Ivanchev, *Polym. Sci. USSR,* **18,** 2141 (1976).
13. N. Friis and A. E. Hamielec, *J. Appl. Polym. Sci.,* **19,** 97 (1975).
14. D. M. Himmelblau, *Applied Nonlinear Programming,* McGraw-Hill Book Company, New York, 1972.
15. K. J. Kim, W. Liang, and K. Y. Choi, *Ind. Eng. Chem. Res.,* **28,** 131 (1989).
16. M. T. Heffelfinger and M. J. Langsam, *J. Appl. Polym. Sci.,* **30,** 3377 (1985).
17. L. H. García and R. D. Patel, *Macromolecules,* **17,** 1998 (1984).

Received April 26, 1995
Accepted July 29, 1995